



Kinematic and dynamic analysis through the robotic formulation of the clavicle-shoulder joint of a human upper extremity

L. A. Mejía^{a*} • L. F. Osorio^a • C. A. Romero^b

^aFaculty of Applied Mechanical, Technological University of Pereira, Pereira, Colombia

^bFaculty of Technologies, Technological University of Pereira, Pereira, Colombia

Received 08 27 2024; accepted 11 07 2024

Available 06 30 2025

Abstract: This paper presents the kinematic and dynamic modeling of the shoulder-clavicle assembly constituting a four-degrees-of-freedom mechanical system. The models are obtained through robotic concepts and formulations, applied to a specific case of arm abduction with movement in the acceleration and deceleration phase, and compared with its equivalent static model. The influence of a suspended mass at the arm's end is also analyzed. Subsequently, a biomechanical model considering the muscular action of the deltoid muscle is created based on the dynamic model obtained, allowing estimation of the force exerted by the moving muscle.

Keywords: Biomechanics, clavicle-shoulder, deltoid muscle, dynamics, kinematics, robotic formulation.

*Corresponding author.

E-mail address: adriamec@utp.edu.co (L. A. Mejía).

Peer Review under the responsibility of Universidad Nacional Autónoma de México.

1. Introduction

While many studies have analyzed the shoulder joint in abduction under static conditions, they often lack specific estimations of force and neglect the kinetics of movement. The study of the upper extremities from a biomechanical perspective holds significant interest today, both for medical purposes such as rehabilitation and prosthetics and for sports enhancement in high-performance athletes or the sports design industry. Mechanical models play a crucial role in guiding limb rehabilitation processes, designing exoskeletons, or enhancing joint and muscle functionality. The shoulder's behavior is particularly complex due to the involvement of three bones - the scapula, the clavicle, and the humerus - interconnected through four joints: the external-clavicular (EC) joint, which connects the end of the clavicle to the sternum; the acromioclavicular (AC) joint, which connects the scapula through the acromion to the clavicle; the scapulothoracic joint (ET), which allows the scapula to slide over the thorax, and the glenohumeral joint (GH), which connects the head of the humerus with the glenoid fossa of the scapula (Barrientos et al., 2002). It is important to note that natural movements of the shoulder always involve the movement of all the bones. Although the main movement of the arm corresponds to that of the humerus, the movements of the scapula are closely related to those of the arm and are secondary to them.

Numerous studies have focused on shoulder behavior, especially injuries in high-performance athletes. These injuries, often caused by poor technique, falls, or conditions such as rotator cuff syndrome, can lead to pain and functional destabilization of the glenohumeral joint. In Barrientos et al. (2002) and Högfors et al. (1995), a review of state-of-the-art models for studying the kinematics and dynamics of the human shoulder joints is presented, with one of these models implemented to address primary morphological restrictions. However, many of these studies do not account for inertial effects when the system experiences accelerations. A significant portion of the literature examines the shoulder joint in abduction under static conditions (Negrete-Mundo & Torres-Zavala, 2016; Hecker et al., 2021; Knighton et al., 2022; Oizumi et al., 2006), often estimating the deltoid muscle's contribution to the movement without specific force estimations or consideration of movement kinetics. Biomechanical studies of the glenohumeral joint using finite element analysis are widely available in literature. Pathological conditions that may represent significant changes in the biomechanical performance of the shoulder are analyzed in Maldonado et al. (2023) and the effect of loads on the mechanical response of the shoulder is analyzed in Yang et al. (2023). In these studies, the results depend on the correct selection of the boundary conditions that include,

among others, muscle forces. Force values obtained from literature and databases are the input for these studies, so it is necessary to complement the data for both static and dynamic loads.

This study aims to create a kinematic and dynamic model of the clavicle-shoulder system using robotic formulation to incorporate movement kinetics. The model is tested for abduction movements, with results compared to static models. Additionally, a biomechanical model is developed considering the muscular action of the deltoid muscle. This paper provides detailed discussions on the kinematics, dynamics, and muscular actions of the system.

2. Materials and methods

2.1. Kinematics of the clavicle-shoulder joint

The kinematics and dynamics of the shoulder-clavicle assembly are formulated using the Denavit-Hartenberg (DH) nomenclature and methodology. This systematic procedure assigns local reference systems to the links of a mechanical system, designating the Z axes based on the characteristic axes of the kinematic joint, Figure 1.

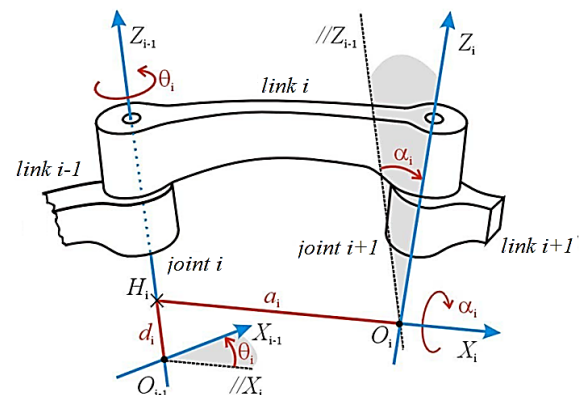


Figure 1. Denavit-Hartenberg parameters.

The sequence of geometric transformations to go from the reference system $\{O_{i-1}\}$ to $\{O_i\}$ is obtained after including an intermediate reference system H_i , so that a rotation of angle θ_i is performed and a translation d_i about the Z axis $i-1$ and then a rotation of the angle α_i and translation a_i about the X axis of the intermediate reference system H_i , which corresponds to X_i . This sequence of movements generates a matrix that allows determining the position and orientation of the reference system of body i in terms of its predecessor $i-1$.

This homogeneous transformation matrix is a function of four parameters α_i , a_i , θ_i , d_i . Three of them are constant and related to the geometry of the elements and the fourth is variable and corresponds to the node variable: for revolute joint, it will be θ_i , and for prismatic pairs d_i of the form:

$${}^{i-1}A_i = \begin{bmatrix} \cos \theta_i & -\cos \alpha_i \sin \theta_i & \sin \alpha_i \sin \theta_i & a_i \cos \theta_i \\ \sin \theta_i & \cos \alpha_i \cos \theta_i & -\sin \alpha_i \cos \theta_i & a_i \sin \theta_i \\ 0 & \sin \alpha_i & \cos \alpha_i & d_i \\ 0 & 0 & 0 & 1 \end{bmatrix} \quad (1)$$

The clavicle or sternoclavicular joint exhibits three degrees of freedom, associated with each cardinal plane: sagittal, frontal, and horizontal, Figure 2. These movements include elevation and descent, protraction and retraction, and axial rotation of the clavicle (Nordin & Frankel, 2004). However, due to limited movements in protraction, retraction, and axial rotation, only the elevation and descent movements are analyzed. The shoulder or acromioclavicular joint, with three degrees of freedom, encompasses ascending and descending rotation, and rotational adjustments in the horizontal and sagittal planes.

Figure 2 illustrates the clavicle-shoulder system with reference systems according to DH notation. The X_{00} - Y_{00} - Z_{00} system is ground-based, with the Z^* axis directed along the vertical axis of the frontal plane. The Z_0 axis corresponds to the clavicle's rotation axis, and Z_1 , Z_2 , and Z_3 define the shoulder joint rotations. The lengths L_1 and L_2 represent the clavicle joint's vertical and horizontal lengths relative to the global system, L_3 is the clavicle's length, and L_b is the arm's length (shoulder- elbow or hand shoulder, depending on how far you want to analyze, assuming the element is completely rigid up to the end-effector).

Table 1 presents the DH parameters for the analyzed system. Notably, the first set of parameters positions and orients the Z_0 reference system relative to the global one but does not include any joint coordinates, as the waist turn is not part of this study's analysis.

Table 1. Denavit-Hartenberg parameters for clavicle-shoulder system.

Reference systems	α_i	a_i	θ_i	d_i
00-0	$-\pi/2$	L_1	0	L_2
0-1	0	L_3	θ_1	0
1-2	$-\pi/2$	0	$\theta_2 - \pi/2$	0
2-3	$-\pi/2$	0	$\theta_3 + \pi/2$	0
3-4	0	0	θ_4	L_b

Direct kinematics. Direct kinematics aims to determine the end effector's position, such as the hand or elbow, from a set of joint coordinates corresponding to each degree of freedom of the system. The clavicle-shoulder assembly is an open kinematic chain, so it can be modeled as a serial robot. Hence, the total homogeneous transformation matrix must be determined from the base reference system $\{O_{00}\}$ to the end effector's reference $\{O_4\}$. By deriving the homogeneous transformation matrices for each shoulder element, the complete transformation matrix is calculated, allowing the end effector's position to be obtained as:

$${}^{00}T_n = \begin{bmatrix} \hat{i} & \hat{j} & \hat{k} & P_x \\ n_x & o_x & a_x & P_y \\ n_y & o_y & a_y & P_z \\ n_z & o_z & a_z & P_z \\ 0 & 0 & 0 & 1 \end{bmatrix} \quad (2)$$

The structure of the homogeneous transformation matrix contains information about the end effector's coordinates (P_x, P_y, P_z) and the unit vectors of its associated reference system. Thus, the end effector's position is calculated as:

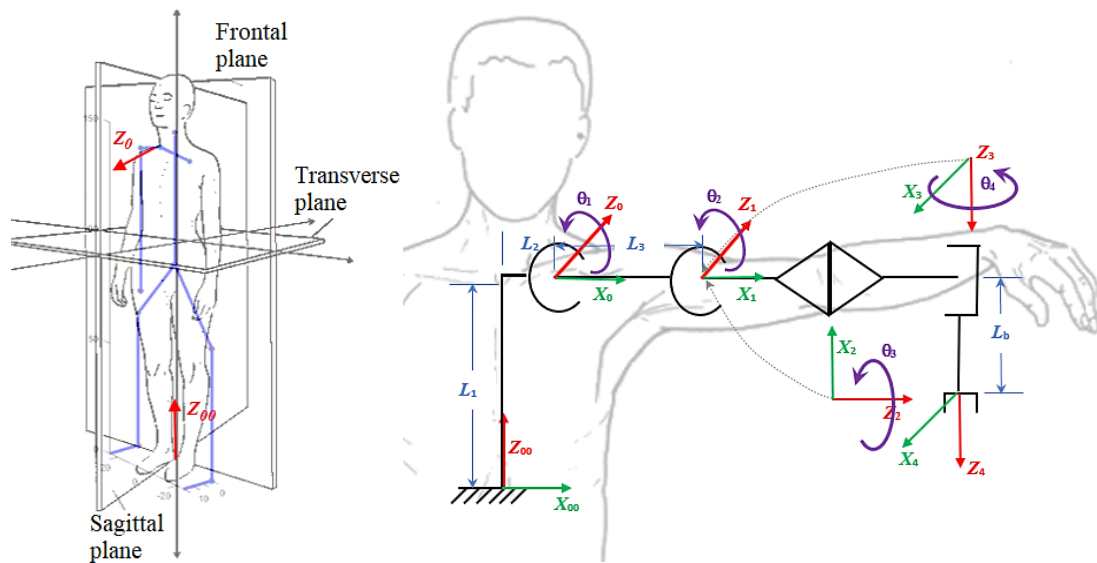


Figure 2. Reference systems of the clavicle-shoulder system.

$$P_x = L_1 + L_3 \cdot \cos \theta_1 + L_b \cdot \sin(\theta_1 + \theta_2) \cdot \cos \theta_3 \quad (3)$$

$$P_y = L_b \cdot \sin \theta_3 \quad (4)$$

$$P_z = L_2 - L_3 \cdot \sin \theta_1 + L_b \cdot \cos(\theta_1 + \theta_2) \cdot \cos \theta_3 \quad (5)$$

Inverse kinematics. Inverse kinematics allows for the determination of node coordinates based on the position and orientation of the end effector. In open kinematic chain systems, it is characterized by multiple possible solutions. For the clavicle-shoulder system, which shares a common node across three degrees of freedom, the Pieper-Roth method is initially applied to determine the value of the first node coordinate θ_1 , before calculating the other angular coordinates. As illustrated in Figure 2, the end-effector resides in the last reference system. Therefore, to obtain the shoulder's position, the distance L_b is moved along axis Z_4 , represented by the vector \hat{a} of the transformation matrix. Thus:

$$P_{\text{shoulder}} = \begin{bmatrix} P_x & P_y & P_z \end{bmatrix} - L_b \begin{bmatrix} a_x & a_y & a_z \end{bmatrix} \quad (6)$$

The shoulder position can also be determined using two transformation matrices:

$$P_{\text{shoulder}} = {}^0A_0 \cdot {}^0A_1 \quad (7)$$

By equating these expressions, the following relationships are derived:

$$P_x - L_b \cdot a_x = L_1 + L_3 \cos \theta_1 \quad (8)$$

$$P_y - L_b \cdot a_y = 0 \quad (9)$$

$$P_z - L_b \cdot a_z = L_2 - L_3 \sin \theta_1 \quad (10)$$

By dividing Eq. 10 by Eq. 8 the first node coordinate is:

$$\theta_1 = \text{atan2}(L_2 - P_z + L_b \cdot a_z, P_x - L_b \cdot a_x - L_1) \quad (11)$$

The other node coordinates are obtained if in Eq. 2 both sides are multiplied by the inverse of the two initial transformation matrices:

$${}^0A_0^{-1} \cdot {}^0A_1^{-1} \cdot {}^0T_n = {}^1A_2 \cdot {}^2A_3 \cdot {}^3A_4 \quad (12)$$

From where it is obtained:

$$P_x \cdot \cos \theta_1 - L_3 - L_1 + P_y \cdot \sin \theta_1 = L_b \cdot \sin \theta_2 \cdot \cos \theta_3 \quad (13)$$

$$L_2 - P_z = -L_b \cdot \cos \theta_2 \cdot \cos \theta_3 \quad (14)$$

$$P_y \cdot \cos \theta_1 - P_x \cdot \sin \theta_1 = L_b \cdot \sin \theta_3 \quad (15)$$

From the previous expressions the node coordinates are found:

$$\theta_2 = \text{atan2}(L_3 + L_1 - P_x \cdot \cos \theta_1 - P_y \cdot \sin \theta_1, L_2 - P_z) \quad (16)$$

$$\theta_3 = \text{asin}\left(\frac{P_y \cdot \cos \theta_1 - P_x \cdot \sin \theta_1}{L_b}\right) \quad (17)$$

Finally, we obtain that:

$$\theta_4 = \text{atan2}(-o_y, n_y) \quad (18)$$

2.2. Dynamics of the clavicle-shoulder complex

For the dynamic analysis of the modeled system, the inverse dynamics method is employed. Newton Euler's formulation is utilized due to the clavicle-shoulder assembly's serial structure, i.e., an open-loop system. This method involves a recursive formulation. Starting from link 1, this method progresses to link n (Figure 3). The detailed Newton-Euler computational algorithm with each step is provided by Yoshikawa (1990).

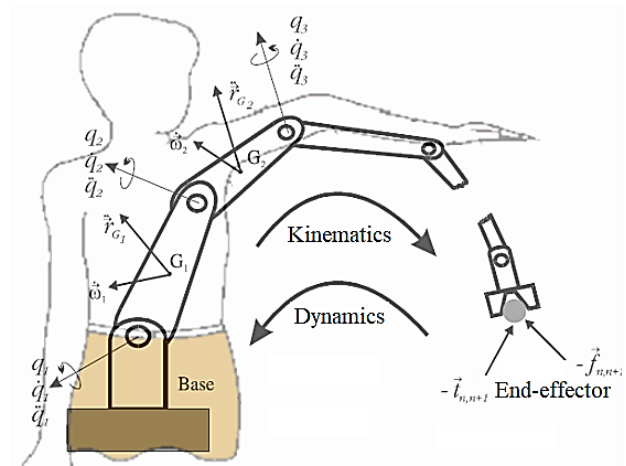


Figure 3. Flow direction in the calculation of the inverse dynamics of a serial robot.

Employing the propagation of velocities and accelerations:

$$\bar{\omega}_i = {}^iR_{i-1} \cdot (\omega_{i-1}^{i-1} + z_0 \dot{\theta}_i) \quad (19)$$

$$\dot{\bar{\omega}}_i = {}^iR_{i-1} \cdot (\dot{\omega}_{i-1} + z_0 \ddot{\theta}_i + \bar{\omega}_{i-1} \times z_0 \dot{\theta}_i) \quad (20)$$

$$\dot{\bar{a}}_i = \dot{\bar{\omega}}_i \times \bar{p}_i + \bar{\omega}_i \times (\bar{\omega}_i \times \bar{p}_i) + {}^i R_{i-1} \cdot \dot{\bar{a}}_{i-1} \quad (21)$$

Being the position vector from the reference system $i-1$ to i expressed in the reference system i and ${}^i R_{i-1}$ the rotation matrix that brings the reference system $i-1$ to coincide with the reference system i and which corresponds to the first three rows and three columns of the inverse matrix ${}^{i-1} A_i$ described in Eq. 1; $z_0 = [0 \ 0 \ 1]^T$.

Using this approach, the accelerations of each element's center of mass are determined, followed by the calculation of forces and torques acting on the element i respect to the robot's base. This process is conducted for all elements from link n to link 1, utilizing inward iterations:

$$\begin{aligned} f_i &= {}^i R_{i+1} \cdot f_{i+1} + m_i a_i \\ n_i &= {}^i R_{i+1} \cdot n_{i+1} + \bar{p}_4 \times f_{i+1} + (\bar{p}_i + \bar{s}_i) \times \\ & m_i a_i + I_i \bar{\omega}_i + \bar{\omega}_i \times I_i \bar{\omega}_i \end{aligned} \quad (22)$$

Subsequently, the torques on each motor are determined:

$$\tau_i = n_i^T ({}^i R_{i+1})^{-1} \cdot z_0 \quad (23)$$

Mechanical model of muscle action. Parameters and conditions are set up to determine the motor torque necessary for the abduction movement, equivalent to the deltoid muscle's action.

The torques required for each joint coordinate are determined using the Newton-Euler formulation. However, the objective is to convert these torques into muscular actions modeled as springs. In this study, the adduction movement of the shoulder while lifting a load is analyzed, considering only the action of the deltoid muscle.

For the development of inverse dynamics, some conditions and parameters must be set up that will determine the motor torque necessary to perform the abduction movement, which will be equivalent to the action of the deltoid muscle. The geometrical parameters used by the dynamic model depend on the anthropometric dimensions of the arm, which vary in individuals based on factors such as ethnicity, age and sex. However, some references (Nordin & Frankel, 2004; Özkaya et al., 2017) provide suggested locations for deltoid anchor points, as well as the dimensions and weight of the arm. A more recent alternative for obtaining geometric parameters involves 3D modeling of anatomical structures through computational segmentations from CT scans and MRI images. This approach, as used in Maldonado et al. (2023), creates a detailed 3D model of a glenohumeral joint to analyze biomechanical changes in the shoulder caused by lesions. This methodology offers the advantage of customizing the geometry of the patient's specific structure, allowing for precise determination of muscle and tendon insertion points.

The inverse dynamics model proposed for the shoulder-clavicle assembly considers the following parameters (Nordin & Frankel, 2004): a) the force produced by the weight of the arm W_b is assumed to be 0.05 times the body weight; b) the force produced through the deltoid muscle acts at a distance L_o of 3 cm for the center of rotation of the shoulder joint (see Figure 4); c) the distance from the center of rotation of the shoulder joint to the point of attachment of the deltoid muscle to the humerus (distance a), which is assumed to be half the distance between the center of rotation of the shoulder joint to the elbow (distance b); d) the dimensions of the arm used for the analysis are dimensions taken from a person of average size. In the scheme, W_{load} is the weight to be lifted, θ is the angle of elevation of the arm, and φ is the angle that the muscle forms with the horizontal which will depend on the elevation of the arm.

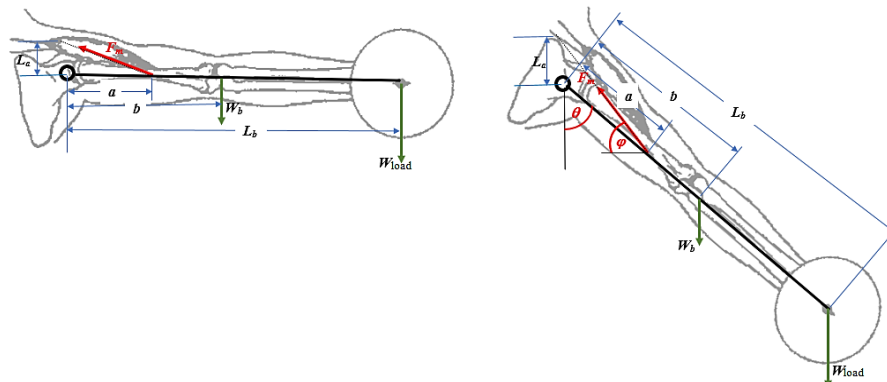


Figure 4. Sizing for the biomechanical model of the deltoid. Source: Adapted from Nordin and Frankel (2004).

The lengths used in the DH parameters, facilitating the determination of the node reference system positions and the end-effector are presented in Table 2. Also included are the weight values used to determine the motor torques.

Table 2. Input data for the analyzed clavicle-shoulder system.

Lengths				Weight	
l	cm	l	cm	W	N
L_1	140	L_2	10	W_{load}	9.81
L_3	14	L_b	64.5	W_b	30.9
L_a	3	a	10		
b	30				

The force exerted by the deltoid muscle will depend on the type of movement analyzed. In static analysis, all the loads acting on the mechanism are balanced, meaning that the motor torque M , obtained from the Newton-Euler algorithm, does not account for inertia, as the linear and angular velocities, as well as accelerations, are zero. In contrast, dynamic analysis considers the kinematic variables of velocity and acceleration associated with the motion.

Once the motor torque has been determined, it is possible to obtain an equivalent system where the movement is generated thanks to the force exerted by the deltoid muscle F_m , like this:

$$F_m = \frac{M_{motor}}{a \cos(\theta_2 - \varphi)} \tag{24}$$

Given the angle φ as:

$$\varphi = \text{atan2}(L_a + a \cos \theta_2, a \sin \theta_2) \tag{25}$$

In a simple spring-type mechanical model, the determination of the equivalent stiffness constant of the deltoid can be determined as:

$$k = F_m / \Delta x \tag{26}$$

where

$$\Delta x = a + L_a - \sqrt{(a \sin \theta_2)^2 + (L_a + a \cos \theta_2)^2} \tag{27}$$

2. Results and discussion

In the analysis proposed in this study, only the action of the deltoid muscle in abduction movement (lateral opening of the arm) is considered. Thus, the nodal variable of the second joint, θ_2 , is known. From direct kinematics, the results of the position are obtained, and through propagation, the velocities

and accelerations of the centers of mass of each element in each arm position are derived.

In the static analysis, as previously mentioned, velocities and accelerations are zero. Therefore, in the dynamic model proposed using Newton-Euler, only the nodal variable θ_2 influences the system. For each value of θ_2 between 0° and 90° , the motor torque M is determined.

The angular velocity of nodal coordinate θ_2 is assumed as a cycloidal function, reaching 90° of abduction in 0.5 seconds, consistent with values reported in the literature (Zapardiel Cortés, 2014; Aragón et al., 2010; Braun et al, 2009); resulting in a maximum speed at the arm's end of 3.87 m/s and a maximum acceleration and deceleration of 25.8 m/s².

The calculated motor torques are presented in Figure 5 for both static and dynamic cases. The graphs show that in the abduction movement, the motor torques in the dynamic instances are lower than those obtained in static cases, even without external load during the acceleration phase. This is because the inertia of the arm and the suspended mass contribute part of the energy associated with movement. However, once deceleration occurs, the required torque increases considerably, approximately 38% more than the referenced value in the static case without load and 42% more when a 1 kg suspended mass is present. The increase in torque is also a consequence of having a mass suspended at arm's end.

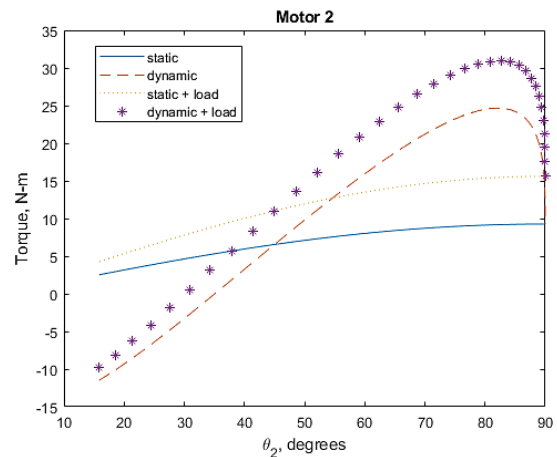


Figure 5. Calculated torques on motor 2 for static and dynamic cases with and without load W_{load} .

Using Eq. 23, the force F_m exerted by the muscle deltoid is determined as a function of the angular position of the arm. Figure 6 shows the variation of said force for static and dynamic analyses. It is observed that during the acceleration phase, the force exerted by the muscle is less than that in the static case. However, once the deceleration phase is reached, the muscle must exert a greater force compared to the static case, increasing by approximately 30% at the point of maximum deceleration. Additionally, the movement changes

the muscle force's behavior as a function of the abduction angle, shifting from linear contraction in the static case to non-linear behavior, where muscle force increases with arm abduction. This is common in sports practice, often leading to injuries.

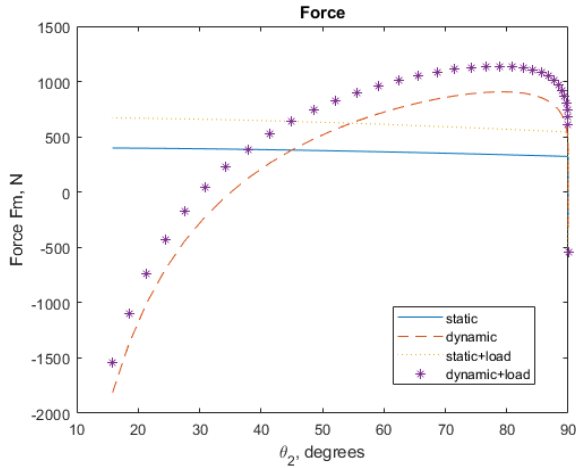


Figure 6. Force exerted by the deltoid muscle in abduction movement in static and dynamic analysis.

The breakdown of the force exerted by the glenohumeral joint on the horizontal and vertical axes is presented in Figure 7.

The vertical force raises the arm and induces rotation, with this action decreasing with greater arm opening in static cases and increasing under kinetic actions. From the graph, it is observed that the horizontal force increases in abduction in both the static and dynamic cases. This component of force is the stabilizer of the shoulder, so large horizontal forces can cause dislocations in the joint. In static cases, the maximum horizontal force occurs near 90° of abduction, further increasing with a suspended mass. Dynamic cases also exhibit maximum horizontal force near 90° of abduction.

Since the force exerted by the deltoid muscle during arm abduction depends on several factors, such as arm angulation, upper limb weight, and additional loads, it is not easy to compare numerical results with previous studies. However, for reports of unloaded forces, Hughes and An (1999) report maximum values of 434 N at abductions of approximately 85°, and Dhein et al. (2020) values of 441 N, consistent with the unloaded values of the static model obtained from the present study, 480 N.

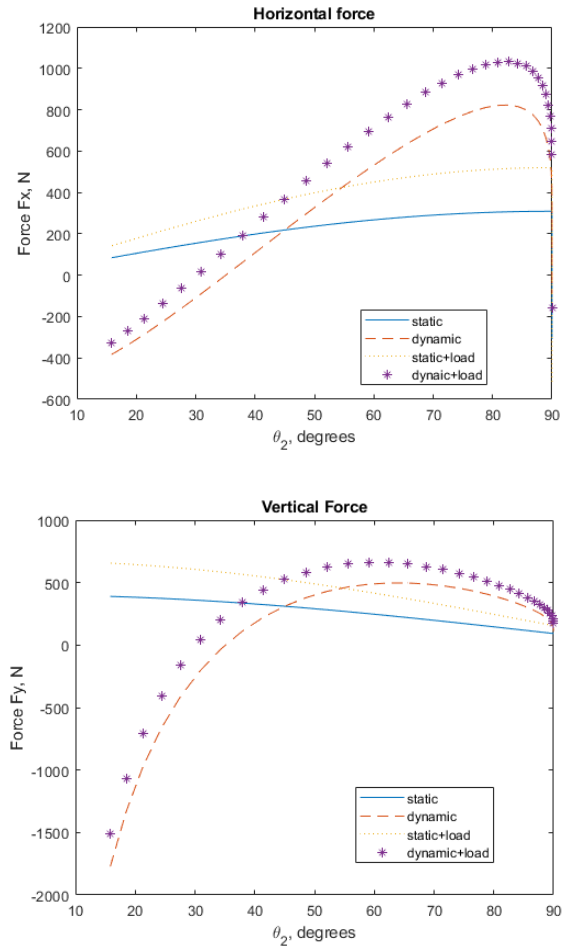


Figure 7. Exerted Horizontal and vertical forces by the glenohumeral joint.

3. Conclusions

The robotic formulations used in the kinematics and dynamics of serial manipulators, as iterative methods with easily implemented algorithms, facilitate the rapid analysis of any open-chain spatial mechanical system, including the human body and its subsystems such as the clavicle-shoulder joints. In this study, the inverse dynamics of the clavicle-shoulder system were successfully modeled and analyzed for arm abduction under both static and dynamic conditions, incorporating acceleration and deceleration profiles typical of sports practice.

Mechanical analysis enables the predictions of estimated values of motor torques necessary for a specific movement under different load conditions, providing insights into the forces acting on muscles. While these predictions offer approximate values, as this modeling approach does not account for all muscles involved in the movement, they provide valuable estimates based on movement characteristics and load variations. In the specific context of

this study, focusing on abduction movement, the deltoid muscle emerges as the primary load-bearing structure. Consequently, the mechanical model was extended to a biomechanical model, enabling the determination of the deltoid muscle's exerted force.

Studies for muscular effort require estimates of muscle contraction forces, which can be preliminarily determined using the methodology established in this work. By integrating mechanics and biomechanics, a comprehensive understanding of the forces and torques involved in shoulder movements, particularly abduction, can be achieved, aiding in injury prevention and rehabilitation strategies, as well as the design of assistive devices and sports equipment.

Considering that the proposed model only included the deltoid muscle for the abduction movement, future work should be done to include other shoulder muscles and to perform analyses for more complex shoulder movements.

Conflict of interest

The authors have no conflict of interest to declare.

Acknowledgments

The author would like to thank the Technological University of Pereira for supporting this work.

Funding

The authors received no specific funding for this work.

References

Aragón, J., Fernandez, J., Gómez, R., Carrasco, A., Mora, J. and Gonzalez, J.L., (2010), *Kinematic analysis of throwing between right and left arm in water-polo*, *International Journal of Medicine and Sciences of Physical Activity and Sports*, vol. 10 (39), pp. 369-379.

Barrientos, G., Quiroz, L. and Saenz, M., (2002), *Numerical simulation of shoulder biomechanics*, *Computational Mechanics*, vol XXI, pp 2505-2518.

Braun, S., Kokmeyer, D., & Millett, P. J. (2009). Shoulder injuries in the throwing athlete. *JBJS*, 91(4), 966-978. <https://doi.org/10.2106/JBJS.H.01341>

Dhein, W., Brodt, G. A., Wagner Neto, E. S., Toledo, J. M. D., Miranda, I. F., & Loss, J. F. (2020). *Muscle force of the shoulder complex with different external loads and movements: a biomechanical simulation analysis*. *Revista Brasileira de Ciência e Movimento*. Vol. 28, no. 1 (2020), p. 127-138.

Hecker, A., Aguirre, J., Eichenberger, U., Rosner, J., Schubert, M., Sutter, R., ... & Bouaicha, S. (2021). Deltoid muscle contribution to shoulder flexion and abduction strength: an experimental approach. *Journal of shoulder and elbow surgery*, 30(2). <https://doi.org/10.1016/j.jse.2020.05.023>

Högfors, C., Karlsson, D., & Peterson, B. (1995). Structure and internal consistency of a shoulder model. *Journal of Biomechanics*, 28(7), 767-777. [https://doi.org/10.1016/0021-9290\(94\)00134-P](https://doi.org/10.1016/0021-9290(94)00134-P)

Hughes, R. E., & An, K. N. (1996). Force analysis of rotator cuff muscles. *Clinical Orthopaedics and Related Research*, 330, 75-83. <https://doi.org/10.1097/00003086-199609000-00010>

Knighton, T. W., Chalmers, P. N., Sulkar, H. J., Aliaj, K., Tashjian, R. Z., & Henninger, H. B. (2022). Anatomic total shoulder glenoid component inclination affects glenohumeral kinetics during abduction: a cadaveric study. *Journal of shoulder and elbow surgery*, 31(10), 2023-2033. <https://doi.org/10.1016/j.jse.2022.03.028>

Maldonado, J. A., Puentes, D. A., Quintero, I. D., González-Estrada, O. A., & Villegas, D. F. (2023). Image-Based Numerical Analysis for Isolated Type II SLAP Lesions in Shoulder Abduction and External Rotation. *Diagnostics*, 13(10), 1819. <https://doi.org/10.3390/diagnostics13101819>

Negrete-Mundo E., & Torres-Zavala A. (2016). Measurement of abduction strength in healthy patients. *Revista Médica del Instituto Mexicano del Seguro Social*. 54(Suppl: 3), 248-253. <https://www.medigraphic.com/cgi-bin/new/resumenl.cgi?IDARTICULO=70887>

Nordin, M., & Frankel, V. H. (2004). *Basic biomechanics of the musculoskeletal system*. Lippincott Williams & Wilkins.

Oizumi, N., Tadano, S., Narita, Y., Suenaga, N., Iwasaki, N., & Minami, A. (2006). Numerical analysis of cooperative abduction muscle forces in a human shoulder joint. *Journal of Shoulder and elbow surgery*, 15(3), 331-338. <https://doi.org/10.1016/j.jse.2005.08.012>

Özkaya, N., Nordin, M., Goldsheyder, D., & Leger, D. (2017). *Fundamentals of biomechanics*, New York: Springer.
<https://doi.org/10.1007/978-3-319-44738-4>

Yang, Z., Xu, G., Yang, J., & Li, Z. (2023). Effect of different loads on the shoulder in abduction postures: A finite element analysis. *Scientific Reports*, 13(1), 9490.
<https://doi.org/10.1038/s41598-023-36049-9>

Yoshikawa, T. (1990). *Foundations of robotics: analysis and control*. MIT press.
<https://doi.org/10.7551/mitpress/3074.001.0001>

Zapardiel Cortés, J. C. (2014). *Isokinetic assessment of the rotator muscles of the shoulder joint complex in beach handball players*, (Doctoral dissertation, Universidad de Alcalá, Spain.)